Theoretical description of low-lying $K^\pi = 1^+$ states in deformed nuclei

O. Civitarese,* Amand Faessler, and R. Nojarov†
Institut für Theoretische Physik, Universität Tübingen, D-7400, Tübingen 1, Federal Republic of Germany
(Received 18 February 1987)

A systematic study of low-lying $K^\pi = 1^+$ states and $M1$ transitions has been performed for the deformed nuclei ^{154}Sm, ^{156}Gd, ^{158}Gd ^{164}Dy, ^{168}Er, and ^{174}Yb within the framework of the quasiparticle random phase approximation in axially symmetric deformed Woods-Saxon potentials. The model Hamiltonian includes a separable quadrupole-quadrupole spin-independent residual interaction. The theoretical results for $0^+ \rightarrow 1^+$ $M1$ transitions in the rare-earth nuclei studied are shown to be in good agreement with the available experimental information.

I. INTRODUCTION

Experimental evidence about the existence of strong $M1$ transitions in deformed nuclei has been reported recently.[1–4] A detailed discussion of the experimental results can be found in the review article by Richter.[5] The experimental data, from (e,e′) reaction on deformed targets in the mass region $150 \leq A \leq 174$,[1–2,4] showed the excitation of $K^\pi = 1^+$ states with $M1$ transition strengths of the order of 1–2 μ_N^2 and energies of the order of 3–4 MeV. Similar evidence about the existence of strong low-lying $M1$ transitions, this time from photoexcitation reactions, has been reported in Ref. 3.

The experimental information has been analyzed from the theoretical side in a number of articles concerned with different models.[6–10] Some of the theoretical descriptions have been already compared with the data in Refs. 1–4. The theoretical descriptions, which have been proposed so far, cover a variety of models, namely the following:

(i) Schematic two-level random-phase-approximation (RPA) calculations of the quadrupole force in a Nilsson potential.[6]

(ii) Deformed RPA calculations with the inclusion of spin-dependent forces in a Woods-Saxon potential.[7]

(iii) A giant-angle dipole mode with single-particle states obtained from the Skyrme interaction.[8]

(iv) A scissor mode, treated in a phenomenological way[9–12] with a microscopic determination of the restoring force.

(v) The interacting boson approximation (IBA).[13] An earlier attempt to describe the physics of strong $M1$ transitions in deformed nuclei has been discussed in terms of a two-rotor model.[14] The picture which emerges from the above mentioned calculations could be summarized in the following:

(i) Strong $M1$ transitions can be expected even at the level of uncorrelated two-quasiparticle states in a deformed potential.

(ii) The transitions are mainly of the isovector type.

(iii) They are described as orbital transitions, affected in a minor sense by a spin-dependent interactions.

(iv) They can be produced by the rotation of protons against neutrons.

Although the interest in the study of these transitions, both experimental and theoretical, grew during the last couple of years, favored by the new data, descriptions of $M1$ transitions within the framework of microscopic models were published some years ago.[15–19] Furthermore, the treatment of isovector vibrations within the framework of the Bohr Hamiltonian was proposed even earlier.[20]

In dealing with the present work, we are motivated, from the theoretical point of view, by the results of Refs. 6 and 7 and 9–12. As in the case of Ref. 6, our interest lies in the fact that the Nilsson plus RPA estimates show a large concentration of strength, even in the case of a small basis. From the results of Ref. 7, a fragmentation of the strength is observed when Woods-Saxon plus RPA calculations are performed, and the predominant orbital character of the transitions is also established. As for Refs. 9–12, the results show a reasonable starting point for a fully microscopical calculation. From the available data we are also interested in a systematic study of the transitions. We have performed, in the present work, a systematic calculation of $M1$ transitions for several deformed nuclei. The calculations were performed at the level of the QRPA (quasi-particle RPA) in axially symmetric Woods-Saxon potentials. Following the results of Ref. 7, we have neglected spin-dependent interactions. This approximation appears to be supported by the experimental results.[4]

The theoretical details are presented in Sec. II; the results of the calculations for the cases of ^{154}Sm, ^{156}Gd, ^{158}Gd, ^{164}Dy, ^{168}Er, and ^{164}Yb are discussed in Sec. III. Some conclusions are drawn in Sec. IV.

II. FORMALISM

In this section we shall briefly describe the theoretical concepts which are relevant for our calculations. To start, we write the intrinsic Hamiltonian

$$H = H_{\rm qp} - \tfrac{1}{2} \sum_{\mu, t_z, t_z'} \chi_{t_z t_z'} \hat{Q}^\dagger_{2\mu}(t_z) \hat{Q}_{2\mu}(t_z') \ , \tag{1}$$

where $H_{\rm qp}$ denotes the unperturbed quasiparticle term, $\hat{Q}_{2\mu}(t_z)$ is the μ component of the quadrupole tensor,

$$\hat{Q}_{2\mu}(t_z)=\sum_{k=1}^{N(t_z)} r_k^2 Y_{2\mu}(\hat{r}_k) , \tag{2}$$

and t_z=p or n denotes either proton or neutron configurations, $N(t_z)$ being the corresponding number of particles. The coupling constants for the neutron-neutron, proton-proton, and neutron-proton channels are χ_{nn}, χ_{pp}, and χ_{np}, respectively. We shall further assume that $\chi_{nn}=\chi_{pp}\neq\chi_{np}$. Since we are interested in the $K^\pi=1^+$ states, the projection μ should be restricted to the values $\mu=\pm1$. The Hamiltonian (1) can be written in the isoscalar and isovector channels by defining the linear combinations

$$\hat{Q}_{21}(m,\tau)=\hat{Q}_{21}(m,\mathrm{n})+(-1)^\tau\hat{Q}_{21}(m,\mathrm{p}) , \tag{3a}$$

where

$$\hat{Q}_{21}(m,t_z)=\tfrac{1}{2}[\hat{Q}^\dagger_{21}(t_z)+m\hat{Q}_{21}(t_z)] , \tag{3b}$$

with $m=\pm1$. The linear combinations (3b) for a given value of t_z define the two intrinsic operators associated with a $K^\pi=1^+$ state, while the isoscalar, $\tau=0$, and isovector, $\tau=1$, operators (3a) define the in- and out-of-phase motion of neutrons and protons, respectively. The index m could be related to the properties of the operators (3b) under time-reversal transformations. In this representation, the Hamiltonian (1) takes the form

$$H=H_{qp}-\tfrac{1}{2}\sum_{m,\tau}\chi(\tau)\hat{Q}^\dagger(m,\tau)\hat{Q}(m,\tau) , \tag{4}$$

where $\chi(\tau)=\chi_{nn}+(-1)^\tau\chi_{np}$. Since we have restricted the angular momentum projection μ to the value $|\mu|=1$, we have performed in (4) the sum over μ and have, for the sake of convenience, omitted this subindex as well as the subindex 2 in the quadrupole operators.

We have to transform, consequently, the quadrupole-quadrupole term of (4) to the quasiparticle basis. We therefore have

$$\hat{Q}(m,t_z)=\sum_{k,i}^{N(t_z)}\{q(ki,mt_z)[A^\dagger(ik,mt_z)+mA(ik,mt_z)] +q(\tilde{k}i,mt_z)[\bar{A}^\dagger(ik,mt_z)+m\bar{A}(ik,mt_z)]\} , \tag{5}$$

where

$$q(ki,mt_z)=-\frac{1}{\sqrt{2}}\langle k|\hat{Q}(m,t_z)|i\rangle U_{ki}(t_z) ,$$
$$q(\tilde{k}i,mt_z)=\frac{1}{\sqrt{2}}\langle k|\hat{Q}(m,t_z)|i\rangle U_{ki}(t_z) , \tag{6}$$

and

$$A^\dagger(ik,mt_z)=\frac{1}{\sqrt{2}}(\alpha^\dagger_{\tilde{i}}\alpha^\dagger_k-m\alpha^\dagger_i\alpha^\dagger_{\tilde{k}})_{(t_z)} ,$$
$$\bar{A}^\dagger(ik,mt_z)=\frac{1}{\sqrt{2}}(\alpha^\dagger_{\tilde{k}}\alpha^\dagger_{\tilde{i}}+m\alpha^\dagger_k\alpha^\dagger_i)_{(t_z)} . \tag{7}$$

The quantities $U_{ki}(t_z)$ are given by

$$U_{ki}(t_z)=(U_kV_i+U_iV_k)_{(t_z)} , \tag{8}$$

in terms of the BCS occupation numbers U and V; $\alpha^\dagger_k$ (α_k) are the quasiparticle creation (annihilation) operators. The states k ($\tilde{k}$) are the one-particle eigenstates of an axially symmetric Woods-Saxon potential, with positive (negative) intrinsic angular momentum projection Ω_k ($-\Omega_k$), expanded in a cylindrical basis. The pair operators $A^\dagger$ and $\bar{A}^\dagger$ fulfill the commutation rules

$$[A(ik,mt_z),A^\dagger(jl,m't_z')]=\delta_{m,m'}\delta_{t_zt_z'}(\delta_{kl}\delta_{ij}+m\delta_{kj}\delta_{il}) ,$$
$$[\bar{A}(ik,mt_z),\bar{A}^\dagger(jl,m't_z')]=\delta_{m,m'}\delta_{t_zt_z'}(\delta_{kl}\delta_{ij}-\delta_{kj}\delta_{il}) , \tag{9}$$
$$[A(ik,mt_z),\bar{A}^\dagger(jl,m't_z')]=[\bar{A}(ik,mt_z),A^\dagger(jl,m't_z')]=0 .$$

The above given definitions are related to those of Pyatov *et al.*[18] The equivalence between the treatment of Ref. 18 and the present one is shown in the Appendix.

We introduce the phonon creation operators

$$\Gamma^\dagger_\nu(m)=\tfrac{1}{2}\sum_{k,i,t_z}[\varphi^{(m)}_{ki}(\nu,t_z)A^\dagger(ik,mt_z) -\phi^{(m)}_{ki}(\nu,t_z)A(ik,mt_z) +\lambda^{(m)}_{ki}(\nu,t_z)\bar{A}^\dagger(ik,mt_z) -\mu^{(m)}_{ki}(\nu,t_z)\bar{A}(ik,mt_z)] , \tag{10}$$

and with them we linearize the Hamiltonian (4), following the standard RPA procedure, in order to determine the energies and amplitudes of the νth phonon. The corresponding dispersion relation is given by the equation

$$1-k(+)[S_\nu(\mathrm{n})+S_\nu(\mathrm{p})] +[k^2(+)-k^2(-)]S_\nu(\mathrm{n})S_\nu(\mathrm{p})=0 , \tag{11}$$

where $k(\pm)=\chi(0)\pm\chi(1)$, and

$$S_\nu(t_z)=4\sum_{k,i}^{N(t_z)}\left\{\frac{q^2(ki,mt_z)E(ki,t_z)}{[E^2(ki,t_z)-W_\nu^2]} +\frac{q^2(\tilde{k}i,mt_z)E(ki,t_z)}{[E^2(ki,t_z)-W_\nu^2]}\right\} , \tag{12}$$

W_ν being the energy of the νth state and

$$E(ki,t_z)=[E(k)+E(i)]_{(t_z)}$$

being the unperturbed energy of the two-quasiparticle configurations. It should be noted that (11) is valid both for $m=+$ and $m=-$, since

$$q^2(ki,mt_z)=q^2(ki,-mt_z)$$

and

$$q^2(\tilde{k}i,mt_z)=q^2(\tilde{k}i,-mt_z) ,$$

and thus the quantities $S_\nu(t_z)$ do not depend on m. It means that the $m=\pm$ phonons are degenerate for a given energy W_ν. Nevertheless, the construction of the intrinsic states requires both types of phonons, as we shall see later.

The corresponding forward- and backward-going amplitudes, which appear in (10), are given by

$$\varphi_{ki}^{(m)}(\nu,t_z)=L_\nu(t_z)\frac{q(ki,mt_z)}{E(ki,t_z)-W_\nu}\ ,$$
$$\phi_{ki}^{(m)}(\nu,t_z)=mL_\nu(t_z)\frac{q(ki,mt_z)}{E(ki,t_z)+W_\nu}\ ,$$
$$\lambda_{ki}^{(m)}(\nu,t_z)=L_\nu(t_z)\frac{q(\tilde{ki},mt_z)}{E(ki,t_z)-W_\nu}\ , \tag{13}$$
$$\mu_{ki}^{(m)}(\nu,t_z)=mL_\nu(t_z)\frac{q(\tilde{ki},mt_z)}{E(ki,t_z)+W_\nu}\ ,$$

where the normalization factor $L_\nu(t_z)$ is given by

$$L_\nu(t_z)=\left[\tfrac{1}{2}W_\nu\left\{S'_\nu(\mathrm{n})+\left[\frac{1-k(+)S_\nu(\mathrm{n})}{k(-)S_\nu(\mathrm{p})}\right]^2 S'_\nu(\mathrm{p})\right\}\right]^{-1/2}$$
$$\times\begin{cases}1 & (t_z=\mathrm{n})\ ,\\ \dfrac{1-k(+)S_\nu(\mathrm{n})}{k(-)S_\nu(\mathrm{p})} & (t_z=\mathrm{p})\ .\end{cases} \tag{14}$$

The quantities $S'_\nu(t_z)$ are defined by

$$S'_\nu(t_z)=\frac{1}{2W_\nu}\frac{\partial}{\partial W_\nu}[S_\nu(t_z)]\ , \tag{15}$$

and, like $S_\nu(t_z)$, they have the same value for $m=\pm$. The phonons $\Gamma_\nu^\dagger(m)$ are normalized, i.e.,

$$1=\tfrac{1}{2}\sum_{k,i,t_z}\{[\varphi_{ki}^{(m)}(\nu,t_z)]^2-[\phi_{ki}^{(m)}(\nu,t_z)]^2$$
$$+[\lambda_{ki}^{(m)}(\nu,t_z)]^2-[\mu_{ki}^{(m)}(\nu,t_z)]^2\}\ , \tag{16}$$

which follows from the commutation relation

$$[\Gamma_\nu(m),\Gamma_{\nu'}^\dagger(m')]=\delta_{\nu,\nu'}\delta_{m,m'}\ . \tag{17}$$

The linearized RPA Hamiltonian can be written as

$$H=H_0+\sum_{m,\nu}W_\nu\Gamma_\nu^\dagger(m)\Gamma_\nu(m)\ , \tag{18}$$

where H_0 is a constant.

As has been pointed out in Refs. 6, 7, 15, and 18, we have to remove the spurious 1^+ state, which in the present context is generated by the action of the angular momentum operator $\hat{J}_+$ on the unperturbed intrinsic ground state. We thus impose the condition

$$[\hat{H},\hat{J}_+]=0\ , \tag{19}$$

in order to get the spurious state at zero energy. Condition (19) relates the matrix elements of the quadrupole operators with the matrix elements of the angular momentum operator $\hat{J}_+$. In the case of a Woods-Saxon potential, this condition can be approximately satisfied by solving the secular equation (11) for $W_\nu=0$. One obtains in this way

$$1-k(+)[S_0(\mathrm{n})+S_0(\mathrm{p})]$$
$$+[k^2(+)-k^2(-)]S_0(\mathrm{n})S_0(\mathrm{p})=0\ . \tag{20}$$

Equation (20) should be considered as the equation which determines one of the two coupling constants $k(+)$ or $k(-)$ in a way consistent with (19). The quantities $S_0(t_z)$ which appear in (20) are given by (12) for $W_\nu=0$. The numerical verification of the relationship between the matrix elements of the quadrupole operator and the matrix elements of the angular momentum operator, in the quasiparticle basis and in a deformed, axially symmetric Woods-Saxon potential, is an interesting problem by itself,[21] but for the present discussion we shall assume, as has been assumed in Refs. 6, 7, and 15, that (20) suffices for the elimination of the spurious 1^+ state from the intrinsic spectrum. A self-consistent treatment of the symmetry restoring mechanism would require the definition of an effective residual interaction.[22] Since the coupling constants $k(+)$ and $k(-)$ are linear combinations of the isoscalar, $\chi(0)$, and isovector, $\chi(1)$, ones, we shall furthermore introduce the ratio $r=\chi(1)/\chi(0)$, as a parameter[6,7] and, in this way, Eq. (20) determines the value of the isoscalar coupling constant and with it the corresponding value, r dependent, of the isovector coupling constant.

Once the structure of the phonon states is determined, by solving the dispersion relation (11) for the energies W_ν with the coupling constants obtained from (20) and by calculating the amplitudes (13), the rotationally invariant wave functions can be written as

$$|IM,K^\pi=1^+,\nu\rangle=\left[\frac{2I+1}{32\pi^2}\right]^{1/2}\sum_{m=\pm}[D^I_{M,1}(\omega)-m(-1)^I D^I_{M,-1}(\omega)]Q_\nu^+(m)|0\rangle\ , \tag{21}$$

where

$$Q_\nu^\dagger(m)=\frac{1}{\sqrt{2}}[\Gamma_\nu^\dagger(m=+)+m\Gamma_\nu^\dagger(m=-)]\ , \tag{22}$$

with $W_\nu\neq 0$.

The correspondence between (22) and the conventional wave function,[23]

$$|IM,K,\nu\rangle=\left[\frac{2I+1}{16\pi^2}\right]^{1/2}[D^I_{M,K}(\omega)\Phi_K(\nu)+(-1)^{I+K}D^I_{M,-K}(\omega)\Phi_{\bar{K}}(\nu)]|0\rangle\ , \tag{23}$$

is straightforward and is based on the realization of the $m=\pm$ phonons as members of an intrinsic time-reversal pair, such as $\Phi_K(\nu)$ and $\Phi_{\bar{K}}(\nu)$, in the notation of Eq. (23).

The tensor components of the intrinsic $M1$ operator read

$$\hat{M}'(M1,\mu)=\left[\frac{3}{4\pi}\right]^{1/2}\mu_N\hat{m}_\mu \ , \tag{24}$$

while in the laboratory frame we have

$$M(M1,\mu)=\sum_\nu D^1_{\mu,\nu}(\omega)\hat{M}'(M1,\nu) \ . \tag{25}$$

The operators $\hat{m}_\mu$ are the tensor components of the magnetic dipole operator,

$$\hat{\mu}=\sum_{t_z} g_l(t_z)\hat{j}(t_z)+\tfrac{1}{2}[g_s(t_z)-g_l(t_z)]\hat{\sigma}(t_z) \ , \tag{26}$$

expanded in the quasiparticle basis, $g_l(t_z)$ and $g_s(t_z)$ are the orbital and spin gyromagnetic factors, respectively, $\mu_N=(e\hbar/2Mc)$ is the Bohr magneton, and $\hat{j}(t_z)$ and $\hat{\sigma}(t_z)$ are the one-body angular momentum and spin operators, respectively. More specifically, we have

$$\hat{m}_{\mu=\pm1}=\mp\frac{1}{\sqrt{2}}\hat{m}_\pm \ , \tag{27}$$

with

$$\hat{m}_\pm=\sum_{k,i,t_z} m_\pm(ki,t_z)\{[A^\dagger(ik,\pm t_z)\mp A(ik,\pm t_z)]+[A^\dagger(ik,\mp t_z)\pm A(ik,\mp t_z)]\}$$
$$+\sum_{k,i,t_z}\tilde{m}_\pm(ki,t_z)\{\mp[A^\dagger(ik,\pm t_z)\mp A(ik,\pm t_z)]\pm[\bar{A}^\dagger(ik,\mp t_z)\pm\bar{A}(ik,\mp t_z)]\} \ ,$$

where

$$m_\pm(ki,t_z)=-\frac{1}{\sqrt{2}}\langle k\mid\hat{m}_\pm\mid i\rangle L_{ki}(t_z), \quad \tilde{m}_\pm(ki,t_z)=\frac{1}{\sqrt{2}}\begin{bmatrix}\langle k\mid m_+\mid\tilde{i}\rangle\\ \text{or}\\ \langle\tilde{k}\mid m_-\mid i\rangle\end{bmatrix}L_{ki}(t_z) \ , \tag{28}$$

and

$$L_{ki}(t_z)=(U_kV_i-U_iV_k)_{(t_z)} \ .$$

After the evaluation of the matrix elements $\langle IM,K^\pi=1^+,\nu\mid\hat{M}(M1,\mu)\mid I=0,M=0,K=0,\text{g.s.}\rangle$, we obtain, for the corresponding transition probabilities in the laboratory frame,

$$B(M1,\nu)\uparrow=\left[\frac{3}{4\pi}\right]\mu_N^2m_\nu^2 \ , \tag{29}$$

where

$$m_\nu=\sum_{\substack{k>i>0\\ t_z}} m_+(ki,t_z)[\varphi^{(-)}_{ki}(\nu,t_z)+\phi^{(-)}_{ki}(\nu,t_z)]+\sum_{\substack{k>i>0\\ t_z}}\tilde{m}_+(ki,t_z)[\lambda^{(-)}_{ki}(\nu,t_z)+\mu^{(-)}_{ki}(\nu,t_z)] \ . \tag{30}$$

It should be noted that the intrinsic matrix element m_ν receives contributions both from the $m=+$ and $m=-$ phonons for a given energy W_ν. Since the terms of (30) are ordered ($\Omega_k>\Omega_i>0$), the amplitudes of the $m=+$ and $m=-$ phonons have been already related and the final expression is written, for convenience, by using only one type of amplitude.

III. RESULTS AND DISCUSSION

In this section we will show the results of our calculations, performed for the deformed nuclei ^{154}Sm, ^{156}Gd, ^{158}Gd, ^{164}Dy, ^{168}Er, and ^{174}Yb.

The single-particle states, both for protons and neutrons and for each nucleus, correspond to the solutions of an axially symmetric Woods-Saxon potential. The parameters of the Woods-Saxon potential are taken from Ref. 24, except for the spin-orbit coupling constant for protons, λ, depending on the mass of the nuclei quoted above. We used $\lambda=19$ for all the nuclei except for ^{158}Gd and ^{164}Dy, where $\lambda=15$. The basis includes states up to the maximum allowed shell number $N=11$. As shown in Ref. 24, the single-particle wave functions are expanded in a cylindrical basis and the states are labeled by their parity, π, and by their angular momentum projection, Ω, along the symmetry axis. In the notation of Sec. III, the single-

TABLE I. Deformation and gap parameters (from Ref. 11) used in the calculations.

Nucleus	β_2	β_4	Δ_n (MeV)	Δ_p (MeV)
^{154}Sm	0.290	0.080	0.95	1.22
^{156}Gd	0.290	0.055	1.02	1.16
^{158}Gd	0.306	0.035	0.97	1.10
^{164}Dy	0.310	0.0	0.91	0.97
^{168}Er	0.306	0.0	0.88	0.98
^{174}Yb	0.290	0.0	0.83	1.04

particle states are denoted by $k=(\Omega_k,\pi_k)$ and the corresponding time-reversed states by $k=(-\Omega_k,\pi_k)$. The quality of the adopted parametrization has been discussed in Ref. 22, where the resulting values for moments of inertia and quadrupole moments are presented.

The deformation parameters and gap energies are given in Table I. They are taken from Ref. 11, where experimental values were adopted for the hexadecapole deformation, while the quadrupole deformation was chosen to reproduce microscopically the experimental charge quadrupole moments. The gap energies were obtained by solving the BCS equations for neighboring nuclei in order to reproduce the experimental even-odd mass differences.

We have performed the QRPA calculations for the $K^\pi=1^+$ states by following the procedure described in Sec. II. To start, we determined for each case the strength of the isoscalar coupling constant, $\chi(0)$, by solving (20). The ratio between the isovector and isoscalar coupling constants was fixed at $r=-3.5$, as Ref. 7. Next, we solved Eq. (11) and verified the accuracy of the procedure by comparing the QRPA energy-weighted sum rule

$$\mathrm{EWSR(QRPA)}=\sum_\nu W_\nu B(M1,\nu)\uparrow , \tag{31}$$

with the corresponding sum rule for two quasiparticle states,

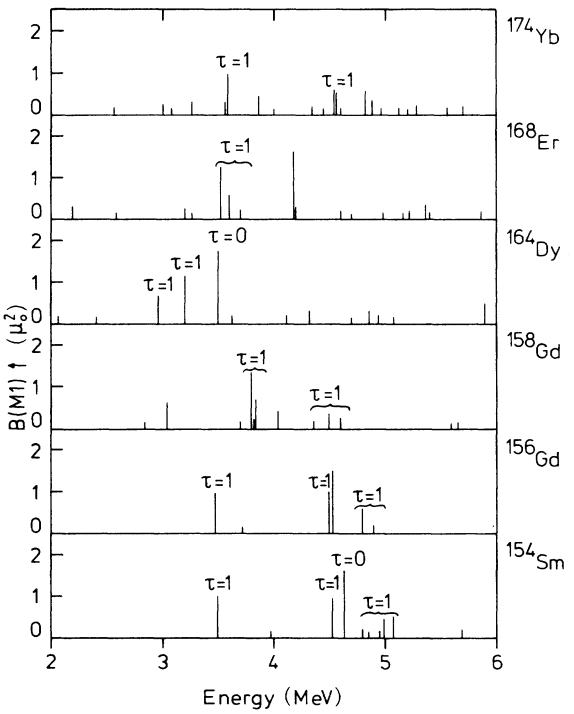

FIG. 1. Transition probabilities $B(M1)$ for the low-lying QRPA states $K^\pi=1^+$ of ^{154}Sm, ^{156}Gd, ^{158}Gd, ^{164}Dy, ^{168}Er, and ^{174}Yb, respectively. The values are given in units of μ_N^2. The dominant isoscalar ($\tau=0$) or isovector ($\tau=1$) character of the states is indicated in the figure. The states where this indication is not inserted have almost equal isovector-isoscalar admixture [comparable absolute values of the two overlaps (33)]. The values of the spin g factors, for protons and neutrons, are given in the text.

$$\mathrm{EWSR(TQP)}=\tfrac{1}{2}\langle 0|[\hat{M}^\dagger,[\hat{H},\hat{M}]]|0\rangle . \tag{32}$$

In all the cases the agreement was of the order of 99%. The dimension of the configuration space was of the order of 1500 quasiparticle pairs.

The results for $B(M1)\uparrow$ transition probabilities are shown in Fig. 1. In this figure we show the low energy region, 2–6 MeV, where strong $M1$ transitions have been observed experimentally. We consider the overlap $I(\tau,\nu)$ of the phonon wave function with the isoscalar and isovector components $\hat{I}(\tau=0,1)$ of the intrinsic angular momentum:

$$\begin{aligned}&\hat{I}(\tau)=\hat{I}_n+(-1)^\tau\hat{I}_p ,\\ &I(\tau,\nu)=\langle\hat{I}(\tau),\Gamma_\nu^\dagger\rangle .\end{aligned} \tag{33}$$

We assign to each state isoscalar, $\tau=0$, or isovector, $\tau=1$, character, when the relative phase of the neutron and proton contributions to the overlaps (33) is, respectively, positive or negative and, moreover, $I(\tau,\nu)$ has larger absolute value than $I(-\tau,\nu)$.

The accumulated $B(M1)$ strengths, in bins of 0.5 MeV, are shown in Fig. 2, for the case of ^{154}Sm. The transition probabilities were calculated with the effective values $g^{\mathrm{eff}}(t_z)=0.70g^{\mathrm{free}}(t_z)$ for the spin gyromagnetic factors. The comparison between the experimental and theoretical values, for the measured strong $M1$ transitions, is shown in Fig. 3. The corresponding energies are shown in Fig. 4. As can be seen from Figs. 3 and 4, the agreement between the data and the theoretical results is a good one. Both the calculated transition probabilities and energies are very near to the experimental values. The dependence of the results on the value of the parameter r is shown in Fig. 5, for the cases of ^{154}Sm and ^{174}Yb, and they do not differ much when r takes the values of -3.5 and -0.5, respectively. Concerning the wave functions for the states which have been compared with the data in Figs. 3 and 4, they are given in Table II.

Let us analyze, briefly, the main features of each transition.

(i) ^{154}Sm: The QRPA results gave a root at $W=3.495$ MeV, which exhausted 2.2% of the EWSR(QRPA), with a transition strength of 0.94 μ_N^2. This state is an isovector

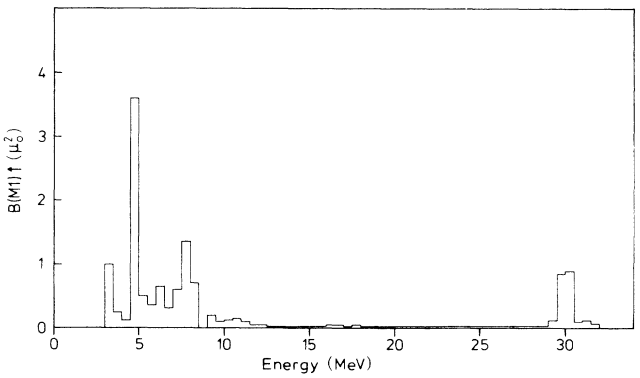

FIG. 2. Histogram corresponding to the theoretical distribution of strength, for $M1$ transitions, in ^{154}Sm.

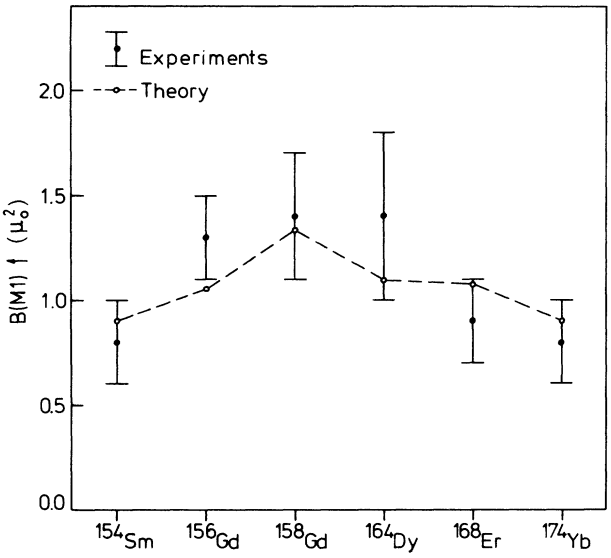

FIG. 3. Comparison between experimental and theoretical results for the low-lying $M1$ transitions analyzed in the text. The experimental values, for the cases of ^{154}Sm, ^{156}Gd, and ^{164}Dy, are taken from Ref. 4, while the corresponding ones for ^{158}Gd, ^{168}Er, and ^{174}Yb are taken from Ref. 2.

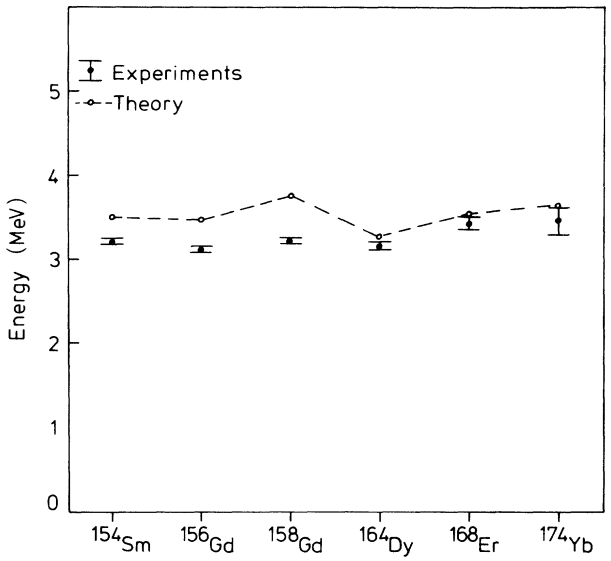

FIG. 4. Comparison between experimental and theoretical values for the energies of the low-lying $K^{\pi}=1^{+}$ states corresponding to the transitions shown in Fig. 3. The experimental values are taken from the references in the caption to Fig. 3.

TABLE II. RPA wave functions of the low-lying $K^{\pi}=1^{+}$ states with largest contributions to the $B(M1)\uparrow$ transition probabilities, as discussed in the text. Only the forward-going amplitudes with absolute values greater than 0.10 are listed. The numbers in square brackets correspond to the asymptotic quantum numbers of the quasiparticle states. They are denoted by the quantum numbers $(Nn_z\Lambda)\Omega$.

Nucleus	Energy (MeV)	Protons	Neutrons
^{154}Sm	3.495	0.93 $[(541)\frac{1}{2},(541)\frac{3}{2}]$	−0.20 $[(532)\frac{3}{2},(523)\frac{5}{2}]$
		0.23 $[(413)\frac{5}{2},(404)\frac{7}{2}]$	
		0.31 $[(541)\frac{3}{2},(532)\frac{5}{2}]$	
^{156}Gd	3.478	−0.63 $[(413)\frac{5}{2},(404)\frac{7}{2}]$	0.47 $[(532)\frac{3}{2},(523)\frac{5}{2}]$
		−0.46 $[(541)\frac{1}{2},(541)\frac{3}{2}]$	
		−0.22 $[(541)\frac{3}{2},(532)\frac{5}{2}]$	
		0.32 $[(532)\frac{5}{2},(523)\frac{7}{2}]$	
^{158}Gd	3.818	−0.92 $[(404)\frac{7}{2},(404)\frac{9}{2}]$	0.30 $[(400)\frac{1}{2},(651)\frac{3}{2}]$
		−0.22 $[(532)\frac{5}{2},(523)\frac{7}{2}]$	
^{164}Dy	3.203	−0.94 $[(532)\frac{5}{2},(532)\frac{3}{2}]$	0.11 $[(633)\frac{7}{2},(624)\frac{9}{2}]$
		−0.29 $[(541)\frac{1}{2},(532)\frac{3}{2}]$	
^{168}Er	3.520	0.99 $[(532)\frac{5}{2},(532)\frac{3}{2}]$	0.10 $[(523)\frac{5}{2},(514)\frac{7}{2}]$
^{174}Yb	3.562	−0.88 $[(532)\frac{3}{2},(532)\frac{5}{2}]$	0.15 $[(521)\frac{3}{2},(512)\frac{5}{2}]$
		−0.20 $[(523)\frac{7}{2},(514)\frac{9}{2}]$	0.11 $[(624)\frac{9}{2},(615)\frac{11}{2}]$
			−0.32 $[(521)\frac{1}{2},(512)\frac{3}{2}]$

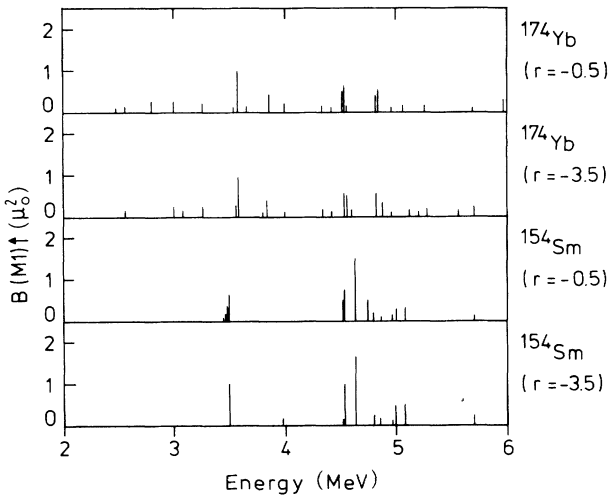

FIG. 5. Results for the theoretical $B(M1)\uparrow$ values, in ^{154}Sm and ^{174}Yb, as a function of the ratio r between the isovector and the isoscalar coupling constants.

one and its wave function is dominated by a proton quasiparticle pair. The experimental results for ^{154}Sm show a $B(M1)\uparrow$ of the order of 0.8 ± 0.2 μ_N^2 at 3.2 MeV.[2,4] We have found, from the theoretical results, also some transitions at energies of the order of 4.5—5 MeV.

(ii) ^{156}Gd: The theoretical results gave one isovector state at 3.478 MeV, with a $B(M1)\uparrow$ of 1.06 μ_N^2, or 2.4% of the EWSR(QRPA). The corresponding experimental values are 3.075 MeV and 1.3 ± 0.2 μ_N^2,[2,4] respectively. In this case, as it is shown in Table I, the wave function is more fragmented than that for the state at 3.495 MeV in ^{154}Sm. Again, in this case, there are strong transitions in the region between 4.5 and 5 MeV.

(iii) ^{158}Gd: We obtained one strong isovector $M1$ transition, at 3.818 MeV, with a $B(M1)\uparrow$ of 1.33 μ_N^2, 3.6% of the EWSR(QRPA), while the data show a transition with 1.4 ± 0.3 μ_N^2 at 3.200 MeV. The low-lying state at about 3 MeV, with a $B(M1)\uparrow$ of the order of 0.5 μ_N^2, is also an isovector one. In this case, the strength in the region between 4.5 and 5 MeV is fragmented. The wave function of this state is concentrated in a proton pair.

(iv) ^{164}Dy: We have obtained one isovector state at 3.203 MeV with a transition strength of 1.10 μ_N^2, or 2.3% of the EWSR(QPRA). The corresponding experimental values are $E=3.110$ MeV, $B(M1)\uparrow=1.5\pm0.3$ μ_N^2,[2] and $E=3.160$ MeV, $B(M1)\uparrow=1.4\pm0.4$ μ_N^2,[4] respectively. The wave function is, in this case also, peaked around a proton pair configuration. The strong transition we obtained at about 3.6 MeV corresponds to an isoscalar state.

(v) ^{168}Er: In this case we obtained one state at 3.520 MeV, with a $B(M1)\uparrow$ of 1.12 μ_N^2, or 2.4% of the EWSR(QRPA). The data are[2] 3.390 MeV and 0.9 ± 0.2 μ_N^2, respectively. This state is, for us, an isovector state built on a single proton pair. As a difference from the cases of ^{158}Gd and ^{164}Dy, the results for ^{168}Er show the presence of one strong transition at about 4.6 MeV, as in the case of ^{154}Sm and ^{156}Gd.

(vi) ^{174}Yb: Our results, for this case, show one isovector state at 3.562 MeV with $B(M1)\uparrow=0.90$ μ_N^2, or 2.1% of the EWSR(QRPA). The corresponding data are[2] 3.555 MeV and 0.8 ± 0.2 μ_N^2, respectively. The wave function is dominated by one proton pair and fragmented in neutron pairs. There is, in this case, a fragmentation of $M1$ strength at energies of the order of 4.5—5 MeV.

The above discussed results show that the strong low-lying $M1$ transitions in deformed nuclei could be interpreted in terms of the excitation of isovector modes. The structure of these modes is, in our model, mainly built on one or two quasiproton pairs with a moderate fragmentation of the quasineutron pair configurations. In addition to the already observed transitions at about 3—4 MeV, the theoretical results show for some cases, other strong transitions in the region between 4 and 5 MeV.

As it is known, from other theoretical attempts,[6–14] the states which we have described above were associated with a collective motion of protons against neutrons.

From the present results, which are on the line of the results presented in Ref. 7, we cannot conclude, in a definite sense, that in all cases the structure of the states meets the requirements of a collective mode. However, the isovector character of the states appears to be confirmed within the framework of the QRPA treatment. Finally, concerning the dominance of orbital or spin contributions to the transition matrix elements, we have found that both contributions are in phase and that the contributions from the spin part of the magnetic dipole operator are comparable to or even larger than the contributions from the orbital part. These conclusions apply, of course, to the transitions we analyzed above.

IV. CONCLUSIONS

In this work we studied, within the QRPA formalism, the main features of the low-lying $M1$ transitions in ^{154}Sm, ^{156}Gd, ^{158}Gd, ^{164}Dy, ^{168}Er, and ^{174}Yb. The calculations were performed in a deformed, axially symmetric Woods-Saxon potential. The residual interactions, of the quadrupole-quadrupole type, do not include a spin-dependent term, since these interactions have already been found to play a minor role.[7] We have analyzed the region between 3 and 4 MeV and the theoretical results are in good agreement with the available experimental information.[1–5] In addition, we have found some other transitions in the region between 4 and 5 MeV, in agreement with the results of Ref. 7. From the analysis of the wave functions, we can conclude that the states have an isovector character, although their collectivity is not so well established because of the dominance of few quasiproton-pair configurations.

An open problem is the interpretation of these states as scissor vibrations. This would request an almost pure orbital excitation of these states. But this seems not to be the case. The states are much less collective than that which a phenomenological description of scissor vibrations would require. They are essentially a superposition of a few two-quasiparticle proton $h_{11/2}$ excitations. It is obvious that for such an excitation the orbital contribution to the $M1$ transition $|g_l l|^2\cong25$, and the isovector part of the spin part, $|\frac{1}{2}(g_p^s-g_n^s)|^2\cong25$, are roughly of

the same order. This is found in the present work. This seems to disagree with recent experimental findings,[4] where inelastic excitations with electrons and protons into these states are performed. The argument goes so that electrons excite both a state of spin and orbital nature, while a proton can only excite a 1^{+} state due to the spin degrees of freedom. (See, for example, the discussion of Faessler.[26]) It seems to us that the larger background in proton scattering due to the possible two step processes in hadron reactions modifies the conclusions. Thus a more accurate measurement of the orbital and the spin contribution to the $M1$ transition is needed. This can be obtained by doing the measurement in the "window" between 200 and 400 MeV proton energy. An even better background reduction can be obtained by using polarized protons in the energy window[27] and doing a double scattering. The protons exciting, via $V_{\sigma\tau}\sigma_1\sigma_2\tau_1\tau_2$, a 1^{+} state can be seen in spin flip, while the two-step processes leading to neighboring states with the strong central force cannot be seen if one looks to the spin flip contribution only. Such a measurement—although difficult—would help to suppress the neighboring background.

This work was supported by the Bundesministerium für Forschung und Technologie and the Alexander von Humboldt Foundation.

APPENDIX

For the sake of completeness, here we shall discuss the equivalence between our formalism and that of Pyatov *et al.*,[18] which is an application of the method due to Marshalek and Weneser.[25] This equivalence could be easily established by defining the relationship between our phonon operators $\Gamma^{\dagger}_{\nu}(m)$ and the $Q^{\dagger}(m)$ phonons of Pyatov *et al.*[18] and the $(P^{(m)},L^{(m)})$ operators of Marshalek and Weneser.[25] The corresponding identities are as follows:

$$P^{(m)}_{\nu}=\frac{\sqrt{W}}{2}[\Gamma^{\dagger}_{\nu}(+)+\Gamma_{\nu}(+)]+m[\Gamma^{\dagger}_{\nu}(-)+\Gamma_{\nu}(-)]\ , \tag{A1}$$

$$L^{(m)}_{\nu}=-\frac{i}{2\sqrt{W}}[\Gamma^{\dagger}_{\nu}(+)-\Gamma_{\nu}(+)]+m[\Gamma^{\dagger}_{\mu}(-)-\Gamma_{\nu}(-)]\ ,$$

$$Q^{\dagger}_{\nu}(m)=\frac{1}{\sqrt{2W}}(P^{(m)}_{\nu}+iW_{\nu}L^{(m)}_{\nu})\ , \tag{A2}$$

and

$$Q^{\dagger}_{\nu}(m)=\frac{1}{\sqrt{2}}[\Gamma^{\dagger}_{\nu}(+)+m\Gamma_{\nu}(+)]\ . \tag{A3}$$

*Permanent address: Department of Physics, University of La Plata, La Plata, Argentina.

†Permanent address: Institute of Nuclear Research and Nuclear Energy, Bulgarian Academy of Sciences, Sofia 1784, Bulgaria.

[1]D. Bohle, A. Richter, W. Steffen, A. E. L. Dieperink, N. Lo Iudice, F. Palumbo, and O. Scholten, Phys. Lett. **137B**, 27 (1984).

[2]D. Bohle, G. Küchler, A. Richter, and W. Steffen, Phys. Lett. **148B**, 260 (1984).

[3]U. E. P. Berg, C. Bläsing, J. Drexler, R. D. Heil, U. Kneissel, W. Naatz, R. Ratzck, S. Schennach, R. Stock, T. Weber, H. Wickert, B. Fischer, H. Hollick, and D. Kollewe, Phys. Lett. **149B**, 59 (1984).

[4]C. Djalali, N. Marty, M. Morlet, A. Willis, J. C. Jourdain, D. Bohle, U. Hartmann, G. Küchler, A. Richter, G. Caskey, G. M. Crawley, and A. Galonsky, Phys. Lett. **164B**, 269 (1985); C. Wesselberg, K. Schiffer, K. O. Zell, P. von Brentano, D. Bohle, A. Richter, G. P. A. Berg, B. Brinkmöller, J. Römer, F. Osterfeld, and M. Yabe, Z. Phys. A **323**, 486 (1986).

[5]A. Richter, in *Nuclear Structure '85,* proceedings of the Niels Bohr Centennial Conference, edited by R. Broglia, G. Hagemann, and B. Herskind (North-Holland, Amsterdam, 1985), p. 469.

[6]D. R. Bes and R. Broglia, Phys. Lett. **137B**, 141 (1984).

[7]I. Hamamoto and S. Aberg, Phys. Lett. **145B**, 163 (1984).

[8]R. R. Hilton, S. Iwasaki, H. J. Mang, P. Ring, and M. Faber (unpublished).

[9]A. Faessler and R. Nojarov, Phys. Lett. **166B**, 367 (1986).

[10]Z. Bochnacki, A. Faessler, and R. Nojarov, J. Phys. G **12**, L47 (1986).

[11]R. Nojarov, Z. Bochnacki, and A. Faessler, Z. Phys. A **324**, 289 (1986).

[12]A. Faessler, R. Nojarov, and S. Zubik, Z. Phys. A **324**, 235 (1986).

[13]S. Pitel, J. Dukelsky, R. P. J. Perazzo, and H. M. Sofia, Phys. Lett. **144B**, 145 (1984).

[14]N. Lo Iudice and F. Palumbo, Phys. Lett. **41**, 1532 (1978).

[15]I. Hamamoto, Nucl. Phys. **A177**, 484 (1971).

[16]S. I. Gabrakov, A. A. Kuliev, N. I. Pyatov, D. I. Salamov, and H. Schulz, Nucl. Phys. **A182**, 625 (1972).

[17]B. L. Birbrair and K. N. Nikolaev, Yad. Fiz. **14**, 705 (1971) [Sov. J. Nucl. Phys. **14**, 397 (1972)].

[18]N. I. Pyatov and M. I. Chernei, Yad. Fiz. **16**, 931 (1972) [Sov. J. Nucl. Phys. **16**, 514 (1973)].

[19]A. A. Kuliev and N. I. Pyatov, Yad. Fiz. **20**, 297 (1974) [Sov. J. Nucl. Phys. **20**, 158 (1975)].

[20]A. Faessler, Nucl. Phys. **185**, 653 (1966).

[21]O. Civitarese, A. Faessler, and R. Nojarov, Phys. Lett. **13B**, 122 (1987).

[22]V. V. Pal'chik and N. I. Pyatov, Yad. Fiz. **32**, 924 (1980) [Sov. J. Nucl. Phys. **32**, 476 (1980)].

[23]A. Bohr and B. R. Mottelson, *Nuclear Structure* (Benjamin, London, 1975), Vol. 2, p. 8—17.

[24]R. Nojarov, J. Phys. G **10**, 539 (1984).

[25]E. R. Marshalek and J. Weneser, Ann. Phys. (Leipzig) **53**, 569 (1969).

[26]A. Faessler, in *Proceedings of the Weak and Electromagnetic Interaction Conference,* Heidelberg, 1986, edited by I. Klapdor (Springer-Verlag, Berlin, 1986), p. 1046.

[27]A. Faessler, in *Proceedings of the Bormio Winter Meeting,* Bormio, 1987, edited by I. Iori (Universidad di Milano, Milano, 1987).